Alfarama Journal of Basic & Applied Sciences

https://ajbas.journals.ekb.eg
ajbas@sci.psu.edu.eg

Faculty of Science Port Said University

http://sci.psu.edu.eg/en/

July 2023, Volume 4 , Issue III

DOI: 10.21608/ajbas.2023.201613.1150

ISSN 2682-275X

Submitted: 21/03/2023

Accepted: 15/05/2023

Pages: 506 - 528

A Seventh-order Perturbational Weighted Essentially Non-oscillatory Scheme for Hyperbolic Conservation Laws

Amr H. Abdalla [1], Martina W. Azer [1,*], Moutaz Ramadan [2]

[1] Department of Physics and Engineering Mathematics, Faculty of Engineering, Port Said University, Egypt.

[2] Department of Mathematics and Computer Science, Faculty of Science, Port Said University, Port Said, Egypt

***Corresponding author: martina_wagdy1993@yahoo.com**

ABSTRACT

This study presents a modified seventh-order weighted essentially non-oscillatory (WENO) finite difference scheme based on the numerical perturbation method established in [1]. The perturbed candidate polynomials of the seventh-order WENO scheme are evolved using a perturbational polynomial of the grid spacing, which modifies the polynomial approximation used for the classical WENO7-Z reconstruction on each candidate stencil. Furthermore, it is found that the new weighted scheme constructed with the new perturbed polynomials candidate has necessary and sufficient conditions for seventh-order convergence that are one order lower than those used by Henrick for the classic WENO scheme with seventh-order convergence, as presented in [2]. As a result, even at critical locations, the new seventh-order WENO scheme, which uses the perturbed polynomials and the same weights as the WENO7-Z scheme as demonstrated in [3], is able to satisfy the necessary and sufficient condition for seventh-order convergence.

The new WENO7-P scheme reduces numerical dissipation in WENO schemes. Numerical examples verify the new scheme's accuracy, low dissipation, and robustness.

Key Words:

Hyperbolic Conservation Laws, WENO Scheme, Perturbational Approach, Seventh-Order WENO Scheme, Runge-Kutta Method, Improved WENO Schemes.

1. INTRODUCTION

Hyperbolic conservation law systems perform a key part in various practical problems including weather prediction, rarefied, gas dynamics, traffic flow models, and numerous other scopes in

engineering and sciences. Thus, solving these sorts of problems by numerical methods, discontinuities can arise in the solution of these problems.

So it's important to use methods that are non-oscillatory near discontinuities and attain high-order accuracy in the smooth regions. Harten [4] established the total variation diminishing (TVD) methods, which are suitable in this regard. After many attempts, Liu et al. [5] proposed the first weighted essentially non-oscillatory (WENO) scheme which is recognized for the solution of hyperbolic conservation laws, particularly for problems involving complex structures. The essentially non-oscillatory (ENO) property of the WENO method near discontinuities has led to its widespread use, as has the WENO method's high and consistent order accuracy in smooth regions to solve the compressible flow cases. As a result, Jiang and Shu [6] formed a traditional smoothness indicator and generalized the WENO schemes structure. Henrick [2] provided a comprehensive investigation of the correctness of Jiang and Shu's fifth-order WENO scheme (WENO-JS) and concluded that it does not attain the ideal order of critical points when the solution's first derivative is concerned. At the same time, They determined what weights are required for fifth-order convergence and developed a new WENO scheme that uses a mapping function to reevaluate the weights of the WENO-JS scheme in order to meet the necessary and sufficient condition (SC) for seventh-order convergence. The SC then guided WENO system weights.

According to the authors' research, the WENO method's numerical results are sensitive to a user-adjustable parameter [7] and can satisfy the SC at critical points of the smooth solution. According to [8], numerous second and third-order global smoothness indicators have been created (even up to eighth-order). Clearly, even at points in which the first derivative equal zero of the smooth solution, these indicators can retrain the seventh order. However, when solving problems involving shock waves, numerical results showed that these higher-order global smoothness indicators may cause oscillations [9]. Conversely, employing the parameter ε prevents the denominator from being equal to zero. Yet, it is remarkable that ε is so critical for altering the solution's accurate sequence. Consequently, a large number of researchers [10, 11, 12] have shown that to achieve the $\mathbf{7}^{\boldsymbol{th}}$-order at critical points, the parameter ε used to figure out the weights of WENO schemes can be seen as a function of the mesh size Δx. However, it is possible to detect that the solutions of those WENO schemes lose the scale in variance property, especially if the reference length is small, in which case Δx will be large and numerical oscillations may occur.

The goal is to achieve the seventh-order accuracy at critical points while keeping dissipation and ENO properties to a minimum in the nearby discontinuities.

Therefore, a weighted scheme to reduce seventh-order convergence constraints is examined in this paper. Gao [13] first introduced the numerical perturbation method (NPM), which solves the convection-diffusion equation. The numerical perturbation method is accomplished by multiplying a perturbational polynomial (a power series of grid intervals) and removing the trimmed error terms from the adapted differential equation to achieve the perturbational polynomial's coefficients. NPM improves scheme accuracy without adding grid points. Using the first-order upwind scheme, Shen [14] created a second-order perturbational finite difference method for the hyperbolic conservation laws. The NPM was extended to the finite volume method by Gao [15], then, Li [16] created a third-order ENO scheme with a higher-order coefficient that utilized the second-order scheme. Yu [17] recently proposed a finite-difference advection system with symplectic perturbations that can reduce phase error.

The WENO scheme's perturbed versions of candidate polynomials are employed to create a new weighted scheme. In addition, this study generalizes and proves a conservative scheme is accurate according to the corollary presented in other studies [18, 19]. Since the perturbed polynomials are of a

higher order than their counterparts, we can combine the NPM with the corollary to reduce the required condition for seventh-order convergence of a seventh-order WENO scheme. At critical points in smooth regions, the perturbational WENO (WENO7-P) scheme, which uses the weights from the WENO7-Z [28] scheme and the perturbed polynomials, can achieve seventh-order accuracy. As for the other parts of the paper, they are as follows: In section 2 the numerical technique is discussed. In Section 3, perturbed candidate polynomials are used to develop a perturbational WENO scheme. In section 4, we discuss the Linear strong-stability-preserving Runge-Kutta time discretization method (ℓSSPRK). In section 5, we will discuss the Central-upwind flux [20]. Many numerical examples are shown in Section 6 to demonstrate the robustness and low dissipation accuracy of the proposed method.

2 NUMERICAL METHODS

The following describes the approximations of systems of hyperbolic conservation laws

$$\begin{aligned} u_t + f(u)_x &= 0 \\ u(x.0) &= u_0(x). \end{aligned} \tag{1}$$

with initial and boundary conditions. In this $u(x,t)$ is the vector of unknown conservative variables and $f(u)$ is the physical flux vector. This paper only considers uniform grids and uses the following notation: let $x_j = j\Delta x, \quad x_{j\pm\frac{1}{2}} = x_j \pm \frac{1}{2}\Delta x, \quad t^n = n\Delta t, u_j^n = u(x_j, t^n)$ and the cell $I_j = [x_{j-\frac{1}{2}}, x_{j+\frac{1}{2}}]$, where Δx and Δt are small spatial and time scales. Consider a control volume in x-space $[x_{j-\frac{1}{2}}, x_{j+\frac{1}{2}}]$. Integrating (1) with respect to x over the volume and keeping the time variable continuous. A system of ordinary differential equations yields the semi-discrete finite volume scheme (ODEs)

$$\frac{d}{dt}u_j(t) = -\frac{1}{\Delta x}\{f_{j+\frac{1}{2}} - f_{j-\frac{1}{2}}\} = L_j(u), \tag{2}$$

where $u_j(t)$ is the space average of the solution in the cell I_j at time t and $f_{j+\frac{1}{2}}$ is the numerical flux at $x = x_{j+\frac{1}{2}}$ and time t.

The computational domain $t \in [0.\infty]$ $andx \in [x_0, x_N]$ is highly regarded in general.

Due to the fact that the solutions of eq. (1) can exhibit discontinuities (shocks) for smooth initial data, cell-averaged discrete quantities are used. In the interval t^n centered around x_j, u_j^n is an approximation to the cell-average solution in the cell $I_j = [x_{j-\frac{1}{2}}, x_{j+\frac{1}{2}}]$.

$$u_j(t) = \frac{1}{\Delta x}\int_{x_{j-\frac{1}{2}}}^{x_{j+\frac{1}{2}}} u(x,t)dx, \quad f_{j+\frac{1}{2}} = f(u_{j+\frac{1}{2}}(t)). \tag{3}$$

Regarding that, the cell average at time t^n, u_j^n are defined from $u_j(t)$, the point values of the function reconstruct are redefined $u(x,t)$ through appropriate nonlinear polynomial interpolation $P_j(x), \quad x \in I_j$. The WENO reconstruction is adopted in the paper. At each cell appearance $x_{j+\frac{1}{2}}$ the reconstruction generates two distinct values for the function $u(x)$, the left state values and the right state value. Therefore, eq.(1) transforms into a sequence of local Riemann Problems (RP) $(j, j+1)$, $i.e.$ eq.(1) conditional upon the initial condition

$$u(x,t^n) = \begin{cases} u_{j+\frac{1}{2}}^L & if \quad x \le x_{j+\frac{1}{2}}, \\ u_{j+\frac{1}{2}}^R & if \quad x_{j-\frac{1}{2}} \le x. \end{cases} \tag{4}$$

In the current WENO scheme, the numerical solution of eq.(2) is advanced in time using the high-order linear strong-stability-preserving Runge-Kutta ($\ell SSPRK$) [21]. The flux $f_{j+\frac{1}{2}}$ at $x_{j+\frac{1}{2}}$ is described as a monotone function of the right and left extrapolated values $u_{j+\frac{1}{2}}^R, \quad u_{j+\frac{1}{2}}^L$ respectively :

$$f_{j+\frac{1}{2}} = f(u_{j+\frac{1}{2}}, t) = f_{j+\frac{1}{2}}(u^L_{j+\frac{1}{2}}, u^R_{j+\frac{1}{2}}). \tag{5}$$

2.1 classical seventh-order WENO Scheme

The polynomial as offered in [22, 3] $p^L_{j+\frac{1}{2}}$ of a WENO scheme of seventh order can be expressed as

$$u^L_{j+\frac{1}{2}} = p_j(x_{j+\frac{1}{2}}) = \sum_{l=0}^{r-1} \omega_l p^{(l)}_{j+\frac{1}{2}}, \quad \sum_{l=0}^{r-1} \omega_l = 1, \quad l = 0,1,2,3. \tag{6}$$

where $p_{j+\frac{1}{2}}$ is the polynomial on the sub-stencil

$$S_k = (x_{i+k-3}, x_{i+k-2}, x_{i+k-1}, x_{i+k}, x_{i+k+1}, x_{i+k+2}, x_{i+k+3})$$

$$\begin{aligned} p^0_{j+\frac{1}{2}} &= \frac{-1}{4}u_{j-3} + \frac{13}{12}u_{j-2} - \frac{23}{12}u_{j-1} + \frac{25}{12}u_j \\ p^1_{j+\frac{1}{2}} &= \frac{1}{12}u_{j-2} - \frac{5}{12}u_{j-1} + \frac{13}{12}u_j + \frac{1}{4}u_{j+1} \\ p^2_{j+\frac{1}{2}} &= \frac{-1}{12}u_{j-1} + \frac{7}{12}u_j + \frac{7}{12}u_{j+1} - \frac{1}{12}u_{j+2} \\ p^3_{j+\frac{1}{2}} &= \frac{1}{4}u_j + \frac{13}{12}u_{j+1} - \frac{5}{12}u_{j+2} + \frac{1}{12}u_{j+3} \end{aligned} \tag{7}$$

ω_k, which is a nonlinear weight, as shown in [3] .

$$\omega_k = \frac{\alpha_k}{\alpha_0+\alpha_1+\alpha_2+\alpha_3}, \quad \alpha_k = d_k(1 + \frac{\tau_7}{(\beta_k+\varepsilon)^2})^q, \quad k = 0,1,2,3. \tag{8}$$

Where d_k are the ideal weights, which equal $d_0 = \frac{1}{35}, \quad d_1 = \frac{12}{35}, \quad d_2 = \frac{18}{35}, \quad d_3 = \frac{4}{35}$.

τ_7 is a global smoothness indicator equal $|\beta_0 - \beta_3|$, and β_k is the smoothness indicator on the substencil S_k. Jiang and Shu [6] calculate a classical formula for β_k .

the accessible format of β_k for the 7th-order WENO scheme$(r = 4)$ that may be proved as

$$\begin{aligned} \beta_0 &= \tfrac{1}{240}(547(u_{j-3})^2 + 7043(u_{j-2})^2 + 11003(u_{j-1})^2 - 9402(u_{j-1})(u_j) \\ &\quad +2107(u_j)^2 - 3882(u_{j-3})(u_{j-2}) + 4642(u_{j-3})(u_{j-1}) - 18542(u_{j-3})(u_j) \\ &\quad +34492(u_{j-2})(u_{j-1}) - 14084)(u_{j-2})(u_j)). \\ \beta_1 &= \tfrac{1}{240}(267(u_{j-2})^2 + 2843(u_{j-1})^2 + 3443(u_j)^2 - 2522(u_j)(u_{j+1}) \\ &\quad 547(u_{j+1})^2 - 1642(u_{j-2})(u_{j-1} + 1602(u_{j-2})(u_j) - 494(u_{j-2}(u_{j+1}) \\ &\quad +11932(u_{j-1})(u_j) - 3844(u_{j-1})(u_{j+1})). \\ \beta_2 &= \tfrac{1}{240}(547(u_{j-1})^2 + 3443(u_j)^2 + 2843(u_{j+1})^2 - 1642(u_{j+1})(u_{j+2}) \\ &\quad +267(u_{j+2})^2 - 25522(u_{j-1})(u_j) + 1922(u_{j-1})(u_{j+1}) - 494(u_{j-1})(u_{j+2}) \\ &\quad +11932(u_j)(u_{j+1}) - 3204(u_j)(u_{j+2})). \\ \beta_3 &= \tfrac{1}{240}(2107(u_j)^2 + 11003(u_{j+1})^2 + 7043(u_{j+2})^2 - 3882(u_{j+2})(u_{j+3}) \\ &\quad +547(u_{j+3})^2 - 9402(u_j)(u_{j+1}) + 7042(u_j)(u_{j+2}) - 1854(u_j)(u_{j+3}) \\ &\quad +34492(u_{j+1})(u_{j+2}) - 9284(u_{j+1})(u_{j+3})). \end{aligned} \tag{9}$$

Note: The right value $u^R_{j+\frac{1}{2}}$ is acquired through symmetry.

From [3], the seventh-order weighted scheme necessary and sufficient conditions for convergence at the seventh-order are found as follows.:

$$\omega^+_k - \omega^-_k = O(\Delta x^4), \tag{10}$$

$$\omega^\pm_k - d_k = O(\Delta x^3). \tag{11}$$

Thus the sufficient condition can be as

$$\omega_k^{\pm} = d_k + O(\Delta x^4). \quad (12)$$

2.2 The 5th-order perturbational WENO scheme

Here, the fifth-order perturbational WENO schemes in [18] and [19] are reviewed. In this subsection, the research proposed the numerical perturbation technique to constitute a WENO scheme. The perturbed scheme will decrease the sufficient condition constraint from the third order to the second order constraint, i.e.

$$\omega_k^{+} = d_k + O(\Delta x^2). \quad (13)$$

The traditional fifth-order WENO scheme employs a 5-points stencil, hereafter referred to as S^5, which is subdivided into three other 3-points stencils S_0, S_1 and S_2 in which the numerical polynomial $p_{j+\frac{1}{2}}$ of a 5th-order WENO scheme can be expressed as

$$u_{j+\frac{1}{2}}^{L} = \hat{p}_j(x_{j+\frac{1}{2}}) = \sum_{k=0}^{r-1} \omega_k p_{j+\frac{1}{2}}^{(k)}, \quad \sum_{k=0}^{r-1} \omega_k = 1, \quad k = 0,1,2. \quad (14)$$

where $\hat{p}_{j+\frac{1}{2}}^{k}$ is the polynomial on the sub-stencil $S_k = (x_{i+k-2}, x_{i+k-1}, x_{i+k}, x_{i+k+1}, x_{i+k+2})$ as cited in[3].

The explicit form of the perturbed function can change the order from second to third order. Hence, it can be derived as follows [1].

$$\tilde{p}_{j+\frac{1}{2}}^{k} = \hat{p}_{j+\frac{1}{2}}^{k} - A_k \frac{-u_{j-2}+2u_{j-1}-2u_{j+1}+u_{j+2}}{2}, \quad (15)$$

where $A_0 = \frac{-1}{4}, A_1 = \frac{1}{12}, A_2 = \frac{-1}{12}$. For more details , see [1].

3 THE CONSTRUCTION OF THE SEVEN-ORDER PERTURBATIONAL WENO SCHEME

The present research suggests a WENO scheme be built using a numerical perturbational approach. The new technique may lessen the sufficient condition's constraint from the fourth order to the third order, i.e.

$$\omega_k^{+} = d_k + O(\Delta x^3). \quad (16)$$

3.1 The development of perturbed candidate polynomials

The Taylor expansions of β_K in the equation. (6) at $x_{i+\frac{1}{2}}$ show

$$\hat{p}_{j+\frac{1}{2}}^{k} = u_{j+\frac{1}{2}} - \frac{1}{24}\frac{\partial^2 u}{\partial x^2}|_{j+\frac{1}{2}}\Delta x^2 + A_k \frac{\partial^4 u}{\partial x^4}|_{j+\frac{1}{2}}\Delta x^4 + O(\Delta x^5). \quad (17)$$

where $A_0 = \frac{-229}{1152}, A_1 = \frac{59}{1152}, A_2 = \frac{-37}{1152}, A_3 = \frac{59}{1152}$.

From [23] Shu and Osher found the presence of constants $a_2, a_4, \dots, a_{2m-2}, \dots$. As:

$$\hat{p}_{j+\frac{1}{2}} = u_{j+\frac{1}{2}} + \sum_{l=1}^{m-1} a_{2l}\Delta x^{2l}\frac{\partial^{2l} u}{\partial x^{2l}}|_{j+\frac{1}{2}} + O(\Delta x^{2m+1}), \quad (18)$$

then this scheme has been further defined to be spatially accurate to the (2m)th order.

For illustration $a_2 = \frac{-1}{24}, a_4 = \frac{7}{5760}, \dots$.

In the relations of coefficients, which Shu offered, are a_{2l} in (18).

$$\sum_{l=0}^{k} \frac{a_{2l}}{2^{2k-2l}(2k-2l+1)!} = 0. \quad a_0 = 1, k = 1,2, \dots, m-1. \quad (19)$$

These equations concluded the seventh-order WENO scheme's accuracy. In addition, they can construct another scheme.

More details review the corollary, presented in [1].

According to the corollary, Eq.(17) shows that the polynomial candidates $\hat{p}^k_{j+\frac{1}{2}}$ are fourth-order accurate. Logically, whether or not the requirements of the weights in Equation (2.1) may be relaxed if all these candidate polynomials are enhanced to fifth-order..
Therefore, The grid spacing perturbational polynomial P_k is used as a basis.

$$P_k = 1 + b_k\Delta x^3 + c_k\Delta x^4 + O(x^5), \tag{20}$$

multiply the perturbed polynomials $\hat{p}^k_{j+\frac{1}{2}}$, and thus obtain the new polynomials $\tilde{p}^k_{j+\frac{1}{2}}$ as

$$\tilde{p}^k_{j+\frac{1}{2}} = P_k\hat{p}^k_{j+\frac{1}{2}}, \tag{21}$$

Based on the corollary in [1], if the following equation holds

$$\hat{p}^k_{j+\frac{1}{2}} = u_{j+\frac{1}{2}} - \frac{1}{24}\frac{\partial^2 u}{\partial x^2}|_{j+\frac{1}{2}}\Delta x^2 + \frac{7}{5760}\frac{\partial^4 u}{\partial x^4}|_{j+\frac{1}{2}}\Delta x^4 + O(\Delta x^5), \tag{22}$$

is satisfied, then $\hat{p}^k_{j+\frac{1}{2}}$ is a seventh-order polynomial. Substituting Eq (17), (20) and (22) into Eq (21), there is

$$\begin{aligned}&(1 + b_k\Delta x^3 + c_k\Delta x^4 + O(x^5))(u_{j+\frac{1}{2}} - \frac{1}{24}\frac{\partial^2 u}{\partial x^2}|_{j+\frac{1}{2}}\Delta x^2 + A_k\frac{\partial^4 u}{\partial x^4}|_{j+\frac{1}{2}}\Delta x^4 + O(\Delta x^5))\\ &= \left(u_{j+\frac{1}{2}} - \frac{1}{24}\frac{\partial^2 u}{\partial x^2}|_{j+\frac{1}{2}}\Delta x^2 + \frac{7}{5760}\frac{\partial^4 u}{\partial x^4}|_{j+\frac{1}{2}}\Delta x^4 + O(\Delta x^5)\right).\end{aligned} \tag{23}$$

Therefore, it is possible at least in theory (let $u_{i+\frac{1}{2}} \neq 0$) to find out that

$$b_k = 0 \tag{24}$$

$$c_k = ((\frac{7}{5760} - A_k)\frac{\partial^4 u}{\partial x^4}|_{j+\frac{1}{2}})/u_{j+\frac{1}{2}}, \tag{25}$$

Supposing $\hat{p}^k_{j+\frac{1}{2}} = u_{j+\frac{1}{2}} + O(\Delta x^2)$ Eq. (17). An approximation of c_k to a high order can be shown as

$$\tilde{c}_k = ((\frac{7}{5760} - A_k)\frac{\partial^4 u}{\partial x^4}|_{j+\frac{1}{2}})/\hat{p}^k_{j+\frac{1}{2}}. \tag{26}$$

It is clear that, there is

$$\tilde{c}_k = c_k + O(\Delta x^3) \tag{27}$$

Thus, the perturbed seventh-order function is obtained as follows:

$$\tilde{p}^k_{j+\frac{1}{2}} = (1 + \tilde{c}_k\Delta x^4)\hat{p}_{j+\frac{1}{2}} = \hat{p}^k_{j+\frac{1}{2}} + \left(\frac{7}{5760} - A_k\right)\frac{\partial^4 u}{\partial x^4}|_{j+\frac{1}{2}}\Delta x^4. \tag{28}$$

On stencil $S_7 = x_{j-3}, x_{j-2}, \dots, x_{j+3}$. $\frac{\partial^4 u}{\partial x^4}|_{j+\frac{1}{2}}$ is offered as

$$\frac{\partial^4 u}{\partial x^4}|_{j+\frac{1}{2}} = \frac{-u_{j-3}+12u_{j-2}-39u_{j-1}+56u_j-39u_{j+1}+12u_{j+2}-u_{j+3}}{6\Delta x^4} + O(\Delta x). \tag{29}$$

By substituting Eq.(29) into Eq. (28), the clear and specific structure of the perturbed function could be shown as

$$\tilde{p}^k_{j+\frac{1}{2}} = \hat{p}^k_{j+\frac{1}{2}} + (\frac{7}{5760} - A_k)\frac{-u_{j-3}+12u_{j-2}-39u_{j-1}+56u_j-39u_{j+1}+12u_{j+2}-u_{j+3}}{6}. \tag{30}$$

As shown:

$$\begin{aligned}
\tilde{p}^0_{j+\frac{1}{2}} &= \tfrac{-1}{4}u_{j-3} + \tfrac{13}{12}u_{j-2} - \tfrac{23}{12}u_{j-1} + \tfrac{25}{12}u_j + \tfrac{1}{30}(-u_{j-3} + 12u_{j-2} - 39u_{j-1} + 56u_j - 39u_{j+1} + 12u_{j+2} - u_{j+3}).\\
\tilde{p}^1_{j+\frac{1}{2}} &= \tfrac{1}{12}u_{j-2} + \tfrac{-5}{12}u_{j-1} + \tfrac{13}{12}u_j + \tfrac{1}{4}u_{j+1} - \tfrac{1}{120}(-u_{j-3} + 12u_{j-2} - 39u_{j-1} + 56u_j - 39u_{j+1} + 12u_{j+2} - u_{j+3}).\\
\tilde{p}^2_{j+\frac{1}{2}} &= \tfrac{-1}{12}u_{j-1} + \tfrac{7}{12}u_j + \tfrac{7}{12}u_{j+1} - \tfrac{1}{12}u_{j+2} + \tfrac{1}{180}(-u_{j-3} + 12u_{j-2} - 39u_{j-1} + 56u_j - 39u_{j+1} + 12u_{j+2} - u_{j+3}).\\
\tilde{p}^3_{j+\frac{1}{2}} &= \tfrac{1}{4}u_j + \tfrac{13}{12}u_{j+1} - \tfrac{5}{12}u_{j+2} + \tfrac{1}{12}u_{j+3} - \tfrac{1}{120}(-u_{j-3} + 12u_{j-2} - 39u_{j-1} + 56u_j - 39u_{j+1} + 12u_{j+2} - u_{j+3}).
\end{aligned} \tag{31}$$

3.2 The weighted form of the WENO7-P Scheme Reconstruction

Employing the perturbed polynomial $\tilde{p}^k_{j+\frac{1}{2}}$. According to Equation (30), the numerical function of a newly weighted scheme is as following:

$$\begin{aligned}\tilde{p}_{j+\frac{1}{2}} &= \sum_{k=0}^{3} \omega_k \tilde{p}^k_{j+\frac{1}{2}} = \sum_{k=0}^{3} \omega_k \hat{p}^k_{j+\frac{1}{2}} + \frac{12\omega_0-3\omega_1+2\omega_2-3\omega_3}{360} \\ &\times \left(-u_{j-3} + 12u_{j-2} - 39u_{j-1} + 56u_j - 39u_{j+1} + 12u_{j+2} - u_{j+3}\right).\end{aligned} \tag{32}$$

where $\omega_0,\ \omega_1,\ \omega_2,\ \omega_3$ correspond to the same weights in WENO7-Z scheme [28] in equ (8).
Then, the conditions that must be achieved for eq.(34) to converge to the seventh order will be worked out. Directly employing the expansion form of $\sum_{k=0}^{3} \omega_k \tilde{p}^k_{j\pm\frac{1}{2}}$ Eqs. (11-15) offered by Borges [3], we have as cited in [24].

$$\begin{aligned}u^L_{j\pm\frac{1}{2}} &= \sum_{k=0}^{3} d_k p^{(k)}_{j\pm\frac{1}{2}} + \sum_{k=0}^{3} (\omega^{\pm}_k - d_k) p^{(k)}_{j\pm\frac{1}{2}} \\ &= [p(x^{(k)}_{j\pm\frac{1}{2}}) + B^{\pm}\Delta x^7 + o(\Delta x^8)] + \sum_{k=0}^{3} (\omega^{\pm}_k - d_k) p^{(k)}_{j\pm\frac{1}{2}}.\end{aligned} \tag{33}$$

after substituting

$$\begin{aligned}u_{j\pm\frac{1}{2}} = \tilde{p}_{j\pm\frac{1}{2}} &= (h_{j\pm\frac{1}{2}} + B^{\pm}\Delta x^7 + O(\Delta x^8)) + \sum_{k=0}^{3} (\omega^{\pm}_k - d_k) \times (h_{j\pm\frac{1}{2}} + A_k \frac{\partial^4 u}{\partial x^4}|_{j\pm\frac{1}{2}} \Delta x^4 + D_k \Delta x^5 \\ &+ O(\Delta x^6)) + \frac{(12\omega^{\pm}_0 - 3\omega^{\pm}_1 + 2\omega^{\pm}_2 - 3\omega^{\pm}_3)}{60} (\frac{\partial^4 u}{\partial x^4}|_{j\pm\frac{1}{2}} \Delta x^4 + O(\Delta x^5)) \\ &= h_{j\pm\frac{1}{2}} + B^{\pm}\Delta x^7 + O(\Delta x^8) + \sum_{k=0}^{3} (\omega^{\pm}_k - d_k) \times (h_{j\pm\frac{1}{2}} + D_k \Delta x^5 + O(\Delta x^6) \\ &+ \frac{(12\omega^{\pm}_0 - 3\omega^{\pm}_1 + 2\omega^{\pm}_2 - 3\omega^{\pm}_3)}{60} O(\Delta x^5).\end{aligned} \tag{34}$$

where $B^+ = B^-$, $A_0 = \frac{-229}{1152}, A_1 = A_3 = \frac{59}{1152}, A_2 = \frac{-37}{1152}$, and $D_0 = \frac{1}{3}\frac{\partial^5 u}{\partial x^5}|_j, D_1 = \frac{-1}{24}\frac{\partial^5 u}{\partial x^5}|_j$, $D_2 = zero, D_3 = \frac{1}{24}\frac{\partial^5 u}{\partial x^5}|_j$,.

Subtraction of the numerical function in Eq.(36)

$$\begin{aligned}\frac{\tilde{u}_{j+\frac{1}{2}} - \tilde{u}_{j-\frac{1}{2}}}{\Delta x} &= u_j + O(\Delta x^7) + \frac{\sum_{k=0}^{3} (\omega^{+}_k - d_k) h_{j+\frac{1}{2}} - \sum_{k=0}^{3} (\omega^{-}_k - d_k) h_{j-\frac{1}{2}}}{\Delta x} \\ &+ \sum_{k=0}^{3} D_k (\omega^{+}_k - \omega^{-}_k) O(\Delta x^4) \\ &+ \sum_{k=0}^{3} (\omega^{+}_k - d_k) O(\Delta x^5) - \sum_{k=0}^{3} (\omega^{-}_k - d_k) O(\Delta x^5) \\ &+ \frac{\left(12(\omega^{+}_0 - \omega^{-}_0) - 3(\omega^{+}_1 - \omega^{-}_1) + 3(\omega^{+}_2 - \omega^{-}_2) - 3(\omega^{+}_3 - \omega^{-}_3)\right)}{60} O(\Delta x^4).\end{aligned} \tag{35}$$

The necessary and sufficient conditions for the 7^{th}-order weighted schemes, equation (33) are derived from equation (35).

$$\omega^{+}_k - \omega^{-}_k = O(\Delta x^3), \tag{36}$$

$$\omega^{\pm}_k - d_k = O(\Delta x^2). \tag{37}$$

When the current necessary and sufficient conditions are compared to the ones derived from the classical WENO schemes, Eq. (15), it is found that the current conditions relax the weight requirements by one order. It is clear, the sufficient condition of the new seventh-order scheme Eq. (34) may be derived as follows:

$$\omega^{\pm}_k = d_k + O(\Delta x^3). \tag{38}$$

3.3 The concluding form of the WENO7-P Scheme reconstruction incorporating ENO property.

The establish of Eq. (32) is formed using the WENO scheme's weighting technique; even so, as the term $u^{(4)}$: $\frac{\partial^4 u}{\partial x^4}|_{j+\frac{1}{2}} = \frac{-u_{j-3} + 12u_{j-2} - 39u_{j-1} + 56u_j - 39u_{j+1} + 12u_{j+2} - u_{j+3}}{6}$,

Scheme Eq. (32) loses the ENO property if it is used in any perturbed candidate polynomial.

It is fortune that, the term $u^{(4)}$ is independent of the classical function $\hat{p}_{j+\frac{1}{2}}$. If a discontinuous solution is found, By reducing the effect of $u^{(4)}$, the scheme achieves the ENO property. This study suggests employing a tunable function to perform this task..

The new scheme's final function in terms of ENO property (WENO7-P) is

$$\begin{aligned}\tilde{p}_{j+\frac{1}{2}} &= \sum_{k=0}^{3} \omega_k \hat{p}^k_{j+\frac{1}{2}} + \frac{\varphi(12\omega_0-3\omega_1+2\omega_2-3\omega_3)}{360} \\ &\times \left(-u_{j-3} + 12u_{j-2} - 39u_{j-1} + 56u_j - 39u_{j+1} + 12u_{j+2} - u_{j+3}\right).\end{aligned} \tag{39}$$

In order for the function φ to work, , it is necessary that

1. The value of φ is a small, if the stencil $S_7 = x_{j-3}, x_{j-2}, \dots, x_{j+3}$ is a discontinuous stencil.
2. The smoothness of stencil S_7, ensures that φ has no impact on the accuracy of the convergence of eq.(32).

As a result of Equation (38), the second condition will be satisfied and it can be expressed as

$$\varphi = 1 + O(\Delta x^3). \tag{40}$$

Here, we examine the function

$$\varphi = 1 - \left(\frac{\tau_7}{\beta_0+\beta_3+\varepsilon}\right)^2. \tag{41}$$

is recommended, where the new τ_7 is the global smoothness indicator

$\tau_7 = |-2\beta_0 - 3\beta_1 + 3\beta_2 + 2\beta_3|$ which its taylor expansion equals

$$\left|\frac{7625}{288}\Delta x^9 u'^{(4)}u'^{(5)} - \frac{26}{3}\Delta x^7 u''u'^{(5)} + \frac{781}{40}\Delta x^7 u'''u'^{(4)} + \Delta x^5 u'u'^{(4)}\right|. \tag{42}$$

In Eq. (9), the indicators of local smoothness are β_0, β_3, ε is a small positive constant is provided, to ensure that the denominator does not equal zero. the function φ can easily meet the design specifications 1) and 3).

The second right-hand term of Eq. (39) is an anti-dissipation term that approximates the fourth derivative of the polynomial p at j+1/2. Consequently, By using a different approach, the new scheme is able to decrease the numerical dissipation of the standard WENO scheme. It is noteworthy to mention that ε is found that the optimal order cannot be attained in WENO scheme in the case that a large constant ε is employed. However, $\varepsilon = 10^{-40}$ smaller values should be used so that the spurious oscillations are reduced. according to the sources [6, 2].

The sound solution of this case: a huge number of researchers adopted ε as a mesh function Δx rather than using the same constant value as suggested in refs. [12, 10]. In order for the WENO-JS scheme to attain the ideal order, regardless of critical points, it was determined that for any design order $(2r-1)$, ε should be $\varepsilon = A\Delta x^2$, where A is unrelated to Δx, the sufficient condition on ε for the WENO-Z scheme to attain the ideal order irrespective of critical points was first introduced by Don and Borges in reference [10] in the form

$$\varepsilon = A\Delta x^m ,$$

where $m(r,q) \geq 2$ is defined as

$$m \leq \Theta(\tau_{2r-1}) - \frac{r-1}{q}$$

where $\Theta(g) = n \leftrightarrow g(\Delta x^n)$ and τ_{2r-1} is the global ideal smoothness indicator. See references [12, 10] for more information.

The seventh-order scheme, for example, the $r = 4, q = 1, and \Theta(\tau_{2r-1}) = 7$ (see in reference [10] table 1). Therefore $m = 4$ that is, $\varepsilon = \Delta x^4$.

3.4 The theoretical analysis of the WENO7-P Scheme

The expansions of Taylor in Eq. (9) at x_j introduces

$$\beta_k = \begin{cases} 0.7cm\Delta x^2(u')^2 + O(\Delta x^4) & if \quad u' \neq 0, u'' \neq 0, \\ 0.7cm\frac{13}{12}\Delta x^4(u'')^2 + O(\Delta x^6) & if \quad u' = 0, u'' \neq 0, \\ \frac{781}{720}\Delta x^6(u''')^2 + O(\Delta x^7) & if \quad u' = 0, , u'' = 0. \end{cases} \tag{43}$$

and the Taylor expansion of τ_7 in eq. (42) given by:

$$\tau_7 = \begin{cases} \left| \frac{7625}{288}\Delta x^9 (u'^{(4)}) - \frac{26}{3}\Delta x^7 u'' u'^{(5)} + \frac{781}{40}\Delta x^7 u''' u'^{(4)} + \Delta x^5 u' u'^{(4)} \right| & \text{if } u' \neq 0, u'' \neq 0 \\ \left| \frac{7625}{288}\Delta x^9 (u'^{(4)}) - \frac{26}{3}\Delta x^7 u'' u'^{(5)} + \frac{781}{40}\Delta x^7 u''' u'^{(4)} \right| & \text{if } u' = 0, u'' \neq 0 \\ \left| \frac{7625}{288}\Delta x^9 (u'^{(4)})(u'^{(5)} + \frac{781}{40}\Delta x^7 u''' u'^{(4)} \right| & \text{if } u' = 0, u'' = 0 \end{cases} \quad (44)$$

When Eqs. (43) and (44) are substituted into Eq. (8), there is

$$\alpha_k = \frac{\tau_7}{\beta_k} = \begin{cases} \frac{1}{(u')^2}\left| \frac{7625}{288}\Delta x^7 (u'^{(4)})(u'^{(5)}) - \frac{26}{3}\Delta x^5 u'' u'^{(5)} + \frac{781}{40}\Delta x^5 u''' u'^{(4)} + \Delta x^3 u' u'^{(4)} \right| & \text{if } u' \neq 0, u'' \neq 0 \\ \frac{12}{13(u'')^2}\left| \frac{7625}{288}\Delta x^5 (u'^{(4)})(u'^{(5)}) - \frac{26}{3}\Delta x^3 u'' u'^{(5)} + \frac{781}{40}\Delta x^3 u''' u'^{(4)} \right| & \text{if } u' = 0, u'' \neq 0 \\ \frac{720}{781(u''')^2}\left| \frac{7625}{288}\Delta x^3 (u'^{(4)})(u'^{(5)}) + \frac{781}{40}\Delta x u''' u'^{(4)} \right| & \text{if } u' = 0, u'' = 0 \end{cases} \quad (45)$$

The power parameter q in the definition of weights eq. (8) affects the convergence order of the seventh-order WENO (WENO7-Z) scheme at critical points; for instance, the seventh-order accuracy if the power q takes the value of 1 and 3.

This q has an impact on the optimal order of convergence. Therefore $q = 1$ is employed in order to retrieve the accuracy of the optimal of the seventh-order in smooth regions such as the first order critical point as shown in eq. (45).

It is worth mentioning that $q = 1$ achieves the ideal order in smooth regions in isolation of the critical points. On the other hand, $q = 3$ achieves the ideal order including the critical points as shown in eq. (43), however, it raises dissipation.

In addition, $q = 1$ can satisfy the sufficient condition in the smooth region encompasses the seventh-order, it makes no dissipation.

Equation (42) demonstrates that the sufficient condition Eq. (38) for WENO7-P scheme seventh-order convergence is met. For this reason, the WENO7-P scheme maintains seventh-order accuracy even near critical points. For the purpose of enhancing the WENO7-Z scheme, a number of the high-order global smoothness indicators (GSI) have been presented. Following the above reasoning, if one were to adopt these high-order GSIs and check that the determined weights satisfied the sufficient condition Eq. (13) at critical points, then type schemes that correspond to WENO-Z would be seventh-order accurate. However, numerical results in the following section shows that the aforementioned high-order GSIs, when used in conjunction with the WENO7-P scheme (Eqs. (39), (41), and (42), can further reduce the numerical dissipation..

4 TIME DISCRETIZATION

Equation (2) is a system of time-dependent ODEs that can be solved by any stable ODE solver that maintains the spatial accuracy of the scheme. Utilizing time discretizations of the same order as space discretization is actually advantageous.

The current research uses the SSP for linear problems [25], the linear strong-stability-preserving Runge-Kutta algorithm ℓSSPRK. Gottlieb's ℓSSPRK (m,m-1) method [25] is used in this paper. Its coefficients can be found recursively to the necessary accuracy.

This paper uses Runge-Kutta techniques to solve an ODE system.

$$\frac{du}{dt} = L(u), \tag{46}$$

where $L(u)$ is an approximation to the derivative $(-f(u)_X)$ in the differential equation eq. (1).
This ℓSSPRK $(m, m-1)$ method is offered by:

$$\begin{aligned} u^{(0)} &= u^n, \\ u^{(i)} &= u^{(i-1)} + \tfrac{1}{2}\Delta t L u^{(i-1)}, \quad i = 1, \dots, m-1, \\ u^{n+1} &= u^{(m)} = \textstyle\sum_{k=0}^{m-2} \gamma_{m,k} u^{(k)} + \gamma_{m,m-1}\left(u^{(m-1)} + \tfrac{1}{2}\Delta t L u^{(m-1)}\right). \end{aligned} \tag{47}$$

For the seventh order $(m = 8)$ $\gamma_{m,k}$ are offered by
$\gamma_{8,0} = \frac{2}{15}, \gamma_{8,1} = \frac{2}{7}, \gamma_{8,2} = \frac{2}{9}, \gamma_{8,3} = \frac{4}{15}, \gamma_{8,4} = 0, \gamma_{8,5} = \frac{4}{45}, \gamma_{8,6} = 0, \gamma_{8,7} = \frac{1}{315}$
As for the general nonlinear problems, the ℓ SSPRK $(m, m-1)$ methods are not $o(\Delta t)^{(m-1)}$ no longer.
The stability condition for the above mentioned schemes is $CFL \leq 1$. where $CFL = \max(S_j^n \frac{\Delta t}{\Delta x})_j$ is the Constant number. Here S_j^n is the maximum propagation speed in I_j at time level n.

5 THE CENTRAL-UPWIND FLUX

The researchers recapitulate the derivation of the central-upwind flux given in [26].
The one-dimensional hyperbolic conservation law system is considered..

$$u_t + f(u)_x = 0, \quad t \geq 0, x \in \Omega, \tag{48}$$

its initial condition is

$$u(x, 0) = u_0(x). \tag{49}$$

It is worth mentioning that $u(x,t)$ is the vector of unidentified conservative variables and $f(u)$ is the physical flux vector.
At first, the researchers reconstruct a conservative non-oscillatory piecewise polynomial interpolation $P_j(x), x \in I_j$ from u_j^n for each cell I_j. It is general that the vector-field polynomial is discontinuous at the cell interfaces, $x_{j+\frac{1}{2}}$ and thus their evolution is locally defined through the solutions of generalized Riemann Problems. The dimension of matching Riemann fans is explained through the right and left-sided local speeds of propagation $a_{j+\frac{1}{2}}^{R,L}$ that can be calculated by

$$\begin{aligned} a_{j+\frac{1}{2}}^{R} &= \max\left\{\lambda_N\left(\frac{\partial f\left(u_{j+\frac{1}{2}}^{L}\right)}{\partial u}\right), \lambda_N\left(\frac{\partial f\left(u_{j+\frac{1}{2}}^{R}\right)}{\partial u}\right), 0\right\}, \\ a_{j+\frac{1}{2}}^{L} &= \min\left\{\lambda_I\left(\frac{\partial f\left(u_{j+\frac{1}{2}}^{L}\right)}{\partial u}\right), \lambda_I\left(\frac{\partial f\left(u_{j+\frac{1}{2}}^{R}\right)}{\partial u}\right), 0\right\}. \end{aligned} \tag{50}$$

with $\lambda_1 < \cdots < \lambda_m$ being the eigenvalues of the Jacobian $\frac{\partial f}{\partial u}$.
Values on the right $u_{j+\frac{1}{2}}^{R} = P_{j+1}(x_{j+\frac{1}{2}})$ and the left $u_{j+\frac{1}{2}}^{L} = P_j(x_{j+\frac{1}{2}})$ of the piece-wise interpolant values $P_j(x)$ at the cell interface $x = x_{j+\frac{1}{2}}$ are shown.

If the flux convexity adjustments near u (j+1/2)(R,L), then the formula eq.(50) is wrong in the nonconvex particular instance, and a more precise calculation of a (j+1/2)(R,L) is required. The speeds in eq. (50) can be calculated accurately under these conditions:

$$a_{j+\frac{1}{2}}^{R} = \max_{u \in [u_{j+\frac{1}{2}}^{\min}, u_{j+\frac{1}{2}}^{\max}]} \{f'(u), 0\}, \quad a_{j+\frac{1}{2}}^{L} = \min_{u \in [u_{j+\frac{1}{2}}^{\min}, u_{j+\frac{1}{2}}^{\max}]} \{f'(u), 0\}, \tag{51}$$

when $u_{j+\frac{1}{2}}^{\min} = \min\{u_{j+\frac{1}{2}}^{L}, u_{j+\frac{1}{2}}^{R}\}$. Look at [26] for further explanations.
The central upwind scheme, which is presented semi-discretely in [26], can be expressed as

$$\frac{d}{dt} u_j(t) = -\frac{1}{\Delta x}\{F_{j+\frac{1}{2}} - F_{j-\frac{1}{2}}\} = L_j(u). \tag{52}$$

In eq. (52), the numerical flux is denoted by

$$F_{j+\frac{1}{2}} = \frac{a^R_{j+\frac{1}{2}} f(u^L_{j+\frac{1}{2}}) - a^L_{j+\frac{1}{2}} f(u^R_{j+\frac{1}{2}})}{a^R_{j+\frac{1}{2}} + a^L_{j+\frac{1}{2}}} + \frac{a^R_{j+\frac{1}{2}} a^L_{j+\frac{1}{2}}}{a^R_{j+\frac{1}{2}} - a^L_{j+\frac{1}{2}}} \left[u^R_{j+\frac{1}{2}} - u^L_{j+\frac{1}{2}} \right]. \quad (53)$$

It's important to note that the accuracy of the reconstruction and the solution to the ordinary differential equation is used to determine the scheme's accuracy.

6 NUMERICAL RESULTS

The following schemes are considered:

1. WENO7-Z, is an enhanced version of the 7th-order WENO scheme offered in [27].
2. WENO7-B is the WENO scheme of the seventh-order, described in [22].
3. WENO7-P refers to the seventh order WENO scheme provided here.

For linear problems, we use the ℓ SSPRK $(m, m-1)$ method for time integration, although for nonlinear problems, we switch to the SSPRK method) schemes eqs. (5,4). In the case of linear issues, the value of $\varepsilon = 10^{-6}$ is employed for the traditional WENO schemes, whereas the value $\varepsilon = 10^{-40}$ is utilised in the various schemes with the traditional WENO scheme ideally and choose $CFL = 0.4$. As for the nonlinear examples, the researchers employ the simulation time as $\Delta t = 16\Delta x^4$, observe [3]. According to the above-mentioned problems, the symbol shows the numerical solution while the full line represents the analytical solution.

6.1 Critical point convergence

Example 1:

The scheme's accuracy at the critical points is checked in the following instants.
For the given function

$$u(x) = x^3 + \cos x. \quad (54)$$

We create a comparison between the L^∞ error where $(L^\infty = max_{j=0}|u_{exact} - u_j|)$ and the convergence rate of the various schemes. This function's $u'(0) = 0$ and $u''(0) \neq 0$ explains the scheme's inaccuracy. The errors and the rates of convergence of the various schemes at the critical point x = 0 are presented in table 1. The WENO7-Z and WENO7-P schemes achieve the seventh-order, whereas the WENO7-B scheme converges to the fourth-order, as shown in the same table. Furthermore in the WENO7-P scheme, the errors are nearly classified with those of WENO7-Z scheme or even in a more accurate way at some grid sizes.

N	WENO7-B		WENO7-Z		WENO7-P	
	L^∞ error	L^∞ order	L^∞ error	L^∞order	L^∞ error	L^∞order
1600	6.22E-11		1.96E-14		1.86E-14	
3200	3.86E-12	4.01	1.46E-16	7.07	1.39E-16	7.06
6400	2.41E-13	4.00	1.08E-18	7.08	1.03E-18	7.08
12800	1.51E-14	3.99	7.83E-21	7.11	7.66E-21	7.07

Table 1: Convergence Study

6.2 Tests of Accuracy

Example 2:

According to the equation of the transport

$$f_t + f_x = 0, \quad x \in [-1,1], \quad (55)$$

Using the periodic initial data

$$f(x,0) = \sin(\pi x). \quad (56)$$

On the interval $[-1,1]$ and periodic boundary conditions. At t=1, we compute the solution. Observe that, as time progresses, the solution is always smooth, and thus this example is used to check the rate at which different schemes converge. The L^∞ errors and the CPU usage at $t = 1$ are presented in table (2). Observations indicate that all schemes attain the intended order of accuracy, with WENO7-P being the most accurate in terms of both sizes of the error and the accuracy order. Currently, the scheme's effectiveness is compared to that of others. According to table (2), the CPU time required by the

WENO7-P scheme on a given mesh is approximately 84% of that required by the WENO7-B scheme and 66% of it required by the WENO7-Z scheme. Figure (1) offers the errors versus CPU time for the three different schemes. Obviously, from figure (1), the result explains that WENO7-P scheme requires the smallest CPU time to attain the same accuracy compared with different schemes. Consequently WENO7-P scheme is more efficient than the other schemes.

Method	Mesh	L^{∞}error	L^{∞}order	CPU Time
WENO7-B	10	2.54E-4		4.20E-2
	20	1.89E-6	7.07	1.57E-1
	40	1.41E-8	7.07	6.11E-1
	80	1.06E-10	7.06	2.37E+0
	160	7.94E-13	7.06	88.94E+0
WENO7-P	10	4.45E-5		5.36E-2
	20	3.36E-7	7.08	1.98E-1
	40	2.49E-9	7.07	7.21E-1
	80	1.85E-11	7.07	2.78E+0
	160	1.37E-13	7.07	1.05E+1
WENO7-Z	10	7.76E-6		3.55E-2
	20	5.75E-8	7.08	1.32E-1
	40	4.28E-10	7.07	5.02E-1
	80	3.18E-12	7.07	1.87E+0
	160	2.36E-14	7.07	7.01E+0

Table 2: Convergence study

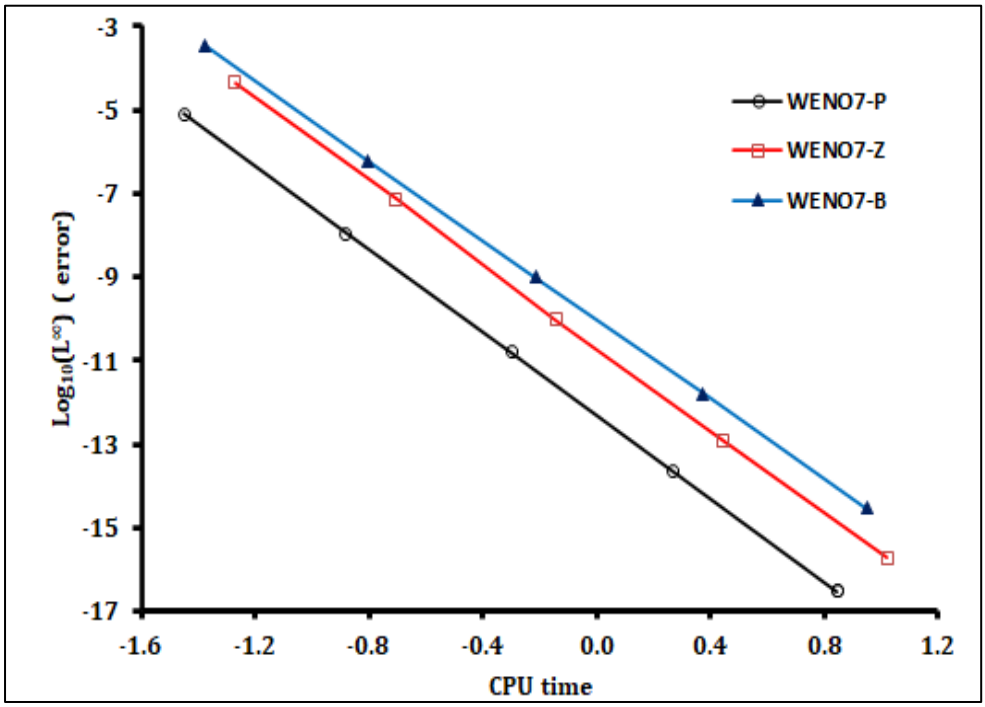

Figure 1: CPU time and L^{∞} curve

6.3 Examples of shocks

Example 3:

Considering the linear equation (55) with this initial condition the correct solutions by the numerical methods will be difficult.

$$u(x,0)=\begin{cases}\frac{1}{6}[G(x,\ z-\delta)+G(x,\ z+\delta)+4G(x,z)], & -0.8\le x\le -0.6,\\ 1, & -0.4\le x\le -0.2,\\ 1-|10(x\ -\ 0.1)|, & 0\le x\le 0.2,\\ \frac{1}{6}[F(x,\ a-\delta)+F(x,a+\delta)+4\,F(x,a)], & 0.4\le x\le 0.6,\\ 0. & otherwise.\end{cases} \quad (57)$$

where $G(x,z)=\exp(-\beta(x-z)^2), F(x,a)=\sqrt{\max(1-\alpha^2(x-a)^2,0}$,and periodic boundary conditions. The values of the constants are $a=0.5, z=-0.7, \delta=0.005, \alpha=10$ and $\beta=(\log 2)/36\delta^2$. At time t = 8 with 200 cells were used to calculate the answers. The results of the WENO7-P scheme are shown in Figure (2). The results with the scheme WENO7-B and WENO7-Z are compared in figures (2) and (3) in [28], Notice that the WENO7-P performs significantly better than the competition in terms of capturing shocks and simulating the top of the semi-ellipse. The errors and CPU time at time t=8 are displayed in table (3). On a given mesh, the WENO7-P scheme uses about 56% less CPU time than the WENO7-B and WENO7-Z schemes combined. Figure (3) presents the L^∞ errors versus CPU time. Clearly, from figure (3), that less CPU time is costed by the WENO7-P scheme to achieve the same accuracy as by the other schemes for this issue. So WENO7-P is more efficient.

N	WENO7-P			WENO7-B			WENO7-Z		
	L^∞ error	L^∞order	CPU	L^∞error	L^∞order	CPU	L^∞error	L^∞ order	CPU
200	7.87E-5		2.13E+0	4.69E-4		3.57E+0	3.59E-4		3.92E+0
400	3.55E-5	1.15	8.68E+0	2.33E-4	1.00	1.51E+1	1.54E-4	1.22	1.52E+1
800	1.71E-5	1.05	3.37E+1	1.17E-4	0.99	6.02E+1	7.63E-5	1.014	5.95E+1
1600	8.37E-6	1.03	1.28E+2	5.71E-5	1.03	2.39E+2	3.73E-5	1.033	2.31E+2

Table 3: Convergence Study

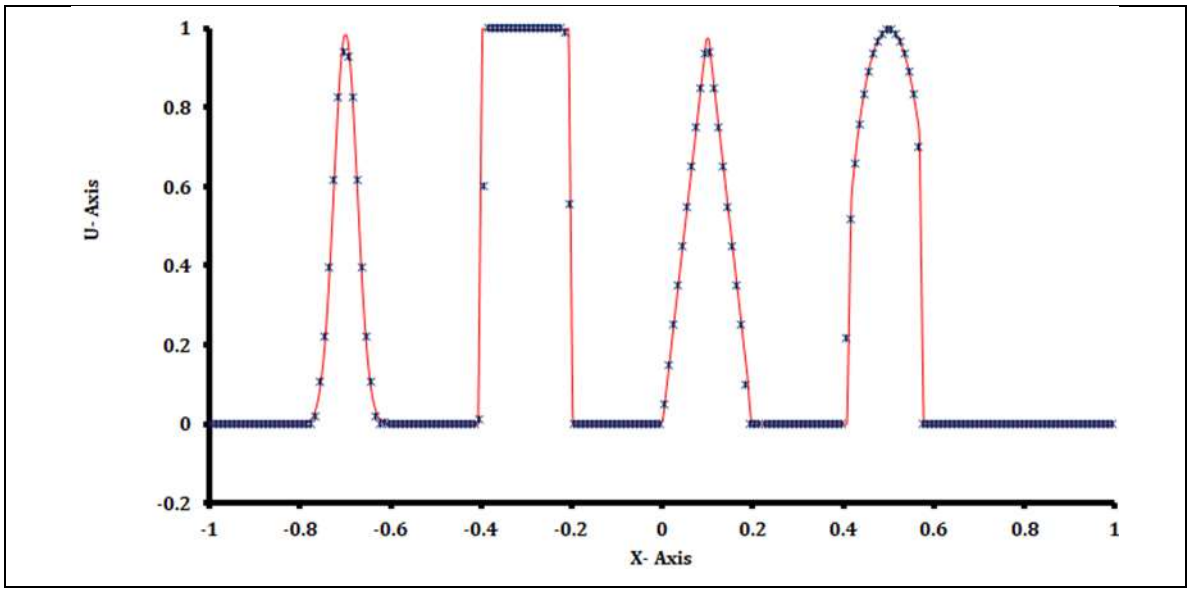

Figure 2: Using WENO7-P scheme at $t=8$

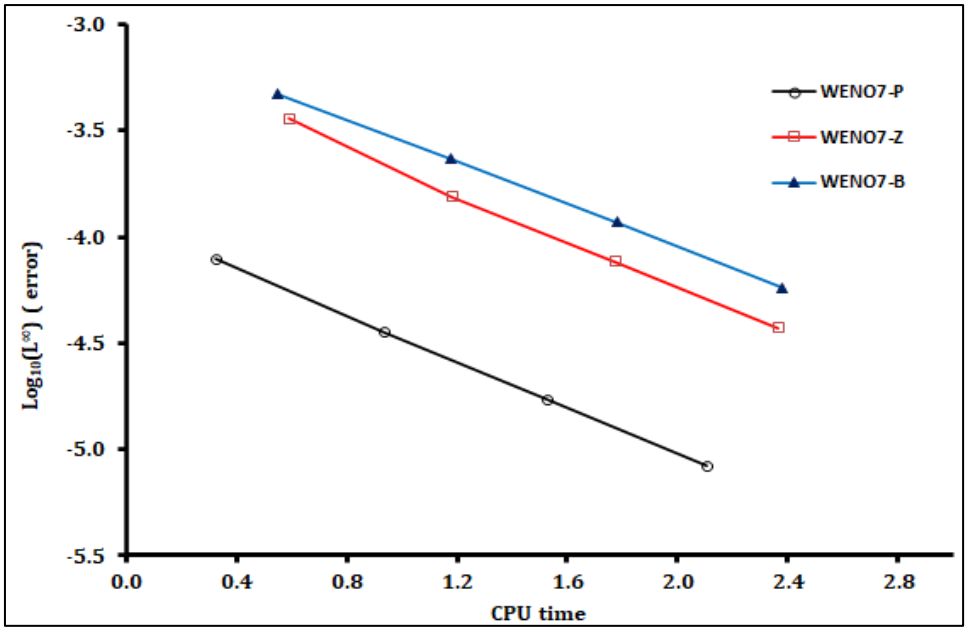

Figure 3: CPU time and L^{∞} curve

Example 4. Burgers (nonlinear equation):
The Burgers equation's numerical solution

$$f_t + (\frac{1}{2}f^2)_x = 0, \quad x \in [0,2], \tag{58}$$

along the initial condition

$$f(x,0) = 0.5 + \sin(\pi x). \tag{59}$$

The results are shown in Figures (4) and (5) at $t = \frac{1.5}{\pi}$ (after the formation of the shock) utilising the WENO7-P and WENO7-Z schemes with a total of N=80 cells respectively. Clearly, the WENO7-P results are nearly clear for the analytical solutions. Drawing a comparison with the performances of all methods, The CPU-L^{∞} error curves are shown in figure (6). It is clear that WENO7-P is more efficient than the others.

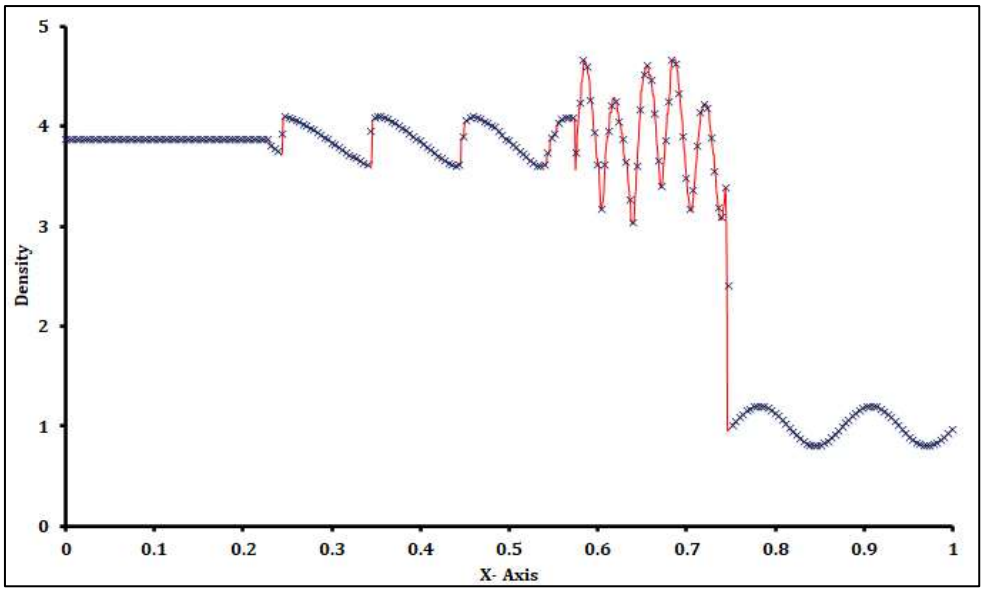

Figure 4: Using WENO7-P scheme

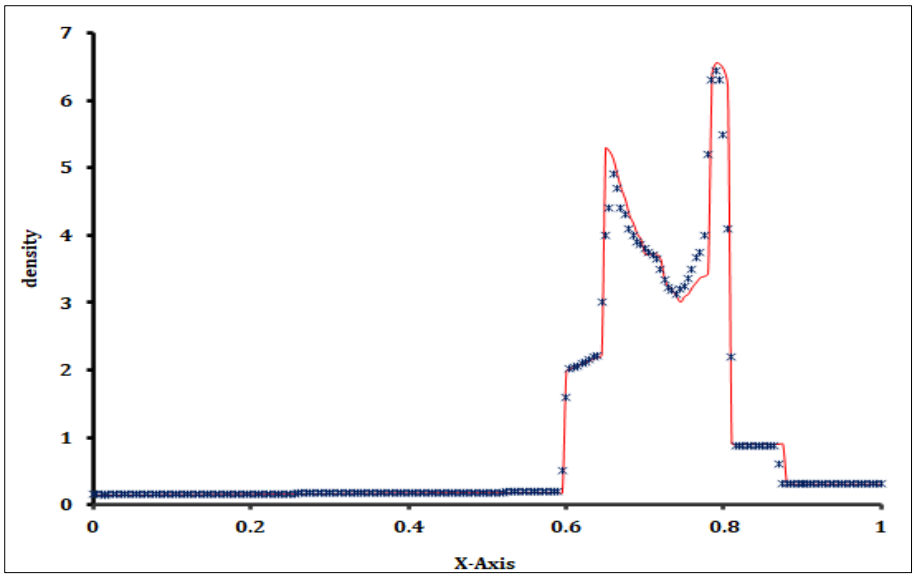

Figure 5: Using WENO7-Z scheme

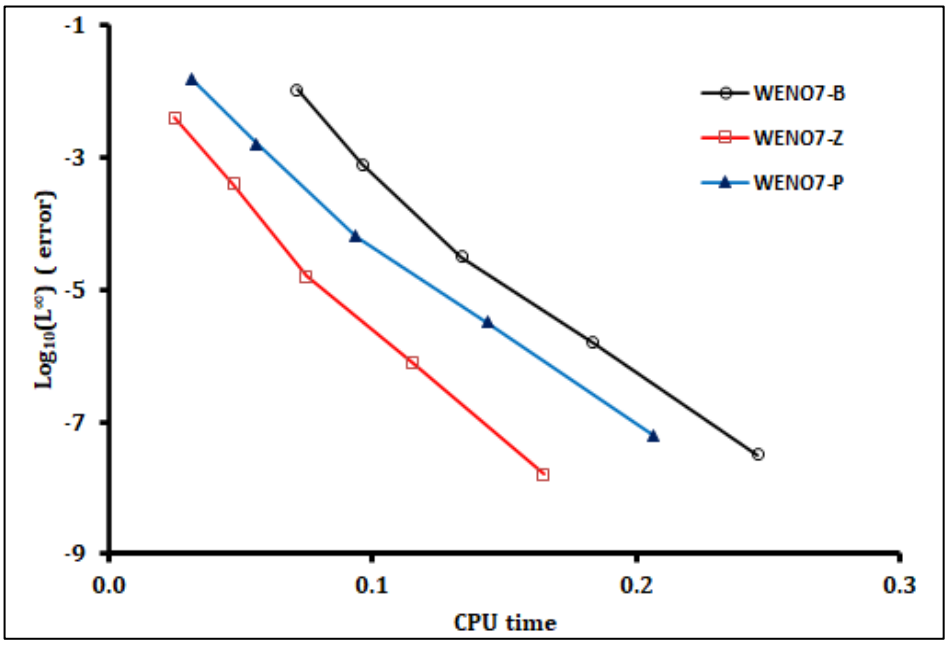

Figure 6: CPU time and L^{∞} curve

6.4 Problem with non-convex flux

Example 5 (Buckley-Leverett Equation)

This instance demonstrates the scheme's performance when employed in the solution of the non-convex fluxes problems.

$$u_t + \left(\frac{4u^2}{4u^2+(1-u)^2}\right)_x = 0, \tag{60}$$

Where the initial condition

$$u(x,0) = \begin{cases} 1, & -0.5 \le x \le 0, \\ 0, & elsewhere. \end{cases} \tag{61}$$

The estimated numerical solution is t=0.4. Its exact solution is a mixture of shock, rarefaction, and contact discontinuity. We observe that some-order schemes do not converge to the proper solution of the entropy for this problem. The numerical results are displayed of WENO7-Z and WENO7-P schemes respectively on the mesh of 80 cells in figures (7,8). Obviously, the two different schemes achieve the correct entropy solution with the ideal resolutions for all the solution's major features. The performances of the schemes are displayed (CPU-L^{∞}error curves in Figure (9). WENO7-P is more effective.

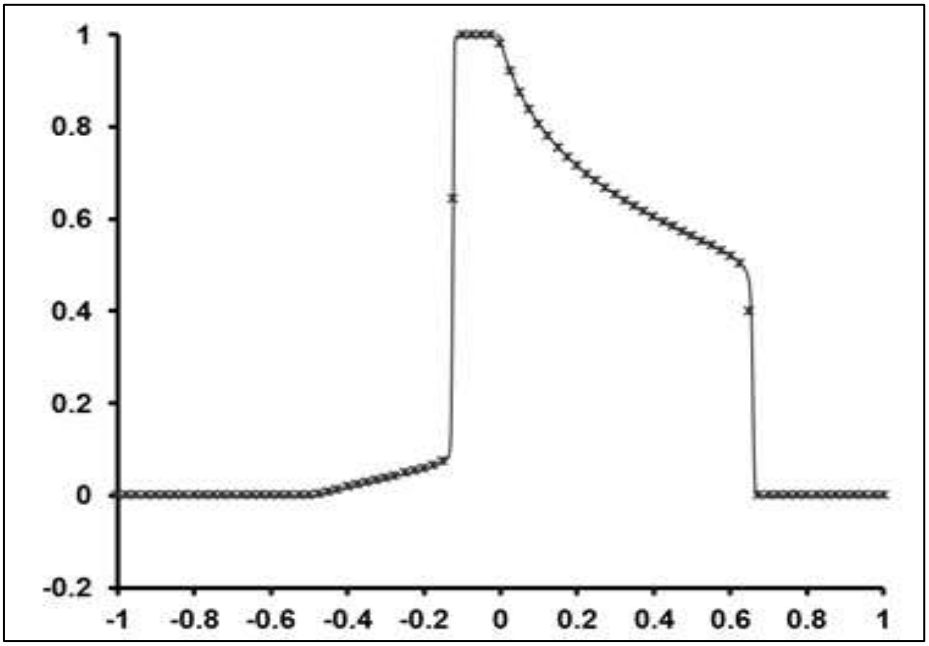

Figure 7: Using WENO7-Z scheme

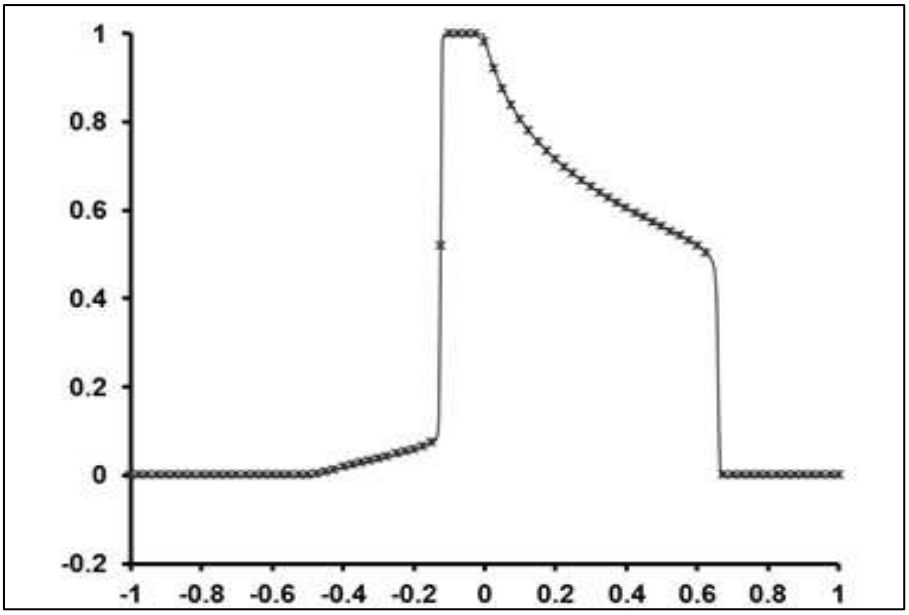

Figure 8: Using WENO7-P scheme

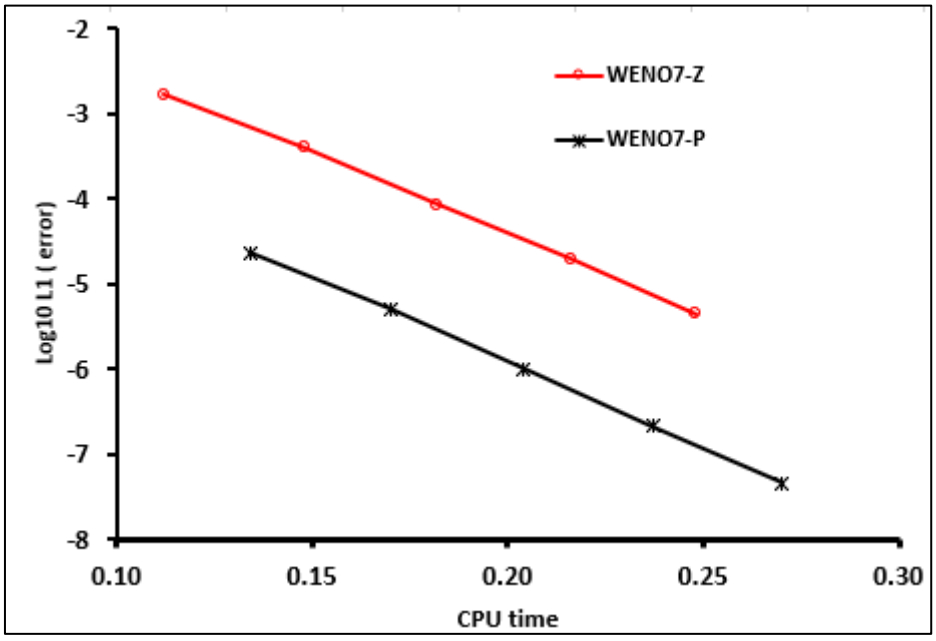

Figure 9: CPU time and L^{∞} curve

6.5 Systems of equations

Regarding the system of gas dynamic Euler equations, we take into account the following:

$$U_t + F(U)_x = 0, \tag{62}$$

Whereas, $U = (\rho, \rho u, E)^T$ and $F(U) = (\rho u, u^2 + P, u(E + P))^T$, where $, u, P, E$ are the density, velocity, pressure, and $E = \frac{1}{2}u^2 + \frac{P}{(\gamma-1)}$ is the total energy and γ is the ratio of specific heat, which is assumed to be 1.4 here.

Example 6. Lax problem:

Equation (62) with two states, left (L) and right (R), as initial conditions

$$(\rho, u, E)^{left} = (0.445,\ 0.311,\ 8.928) \quad and \quad (\rho,\ u,\ E)^{right} = (0.5, 0,\ 1.4275). \qquad (63)$$

it is found discontinuity at $x = 0.5$ at [0,1]. Employing 100 grid points. The results at t=0.13 of the WENO7-P scheme are shown in Figure (10). In comparison to the revised results in [29], the scheme in [29] produced non-physical oscillations close to discontinuities, particularly, close-contact discontinuity, whereas the revised WENO7-P results are more accurate and free of oscillations. Furthermore, in the comparison with WENO7-B and WENO7-Z schemes [28], It is obvious that the perturbation technique is effective and has high accuracy. Figure (11) shows CPU-L^{∞} error curves.

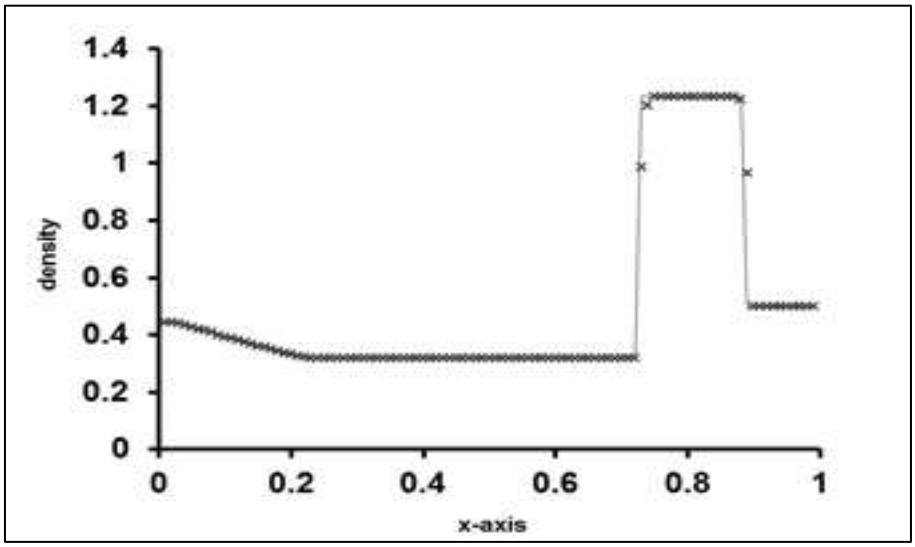

Figure 10: Using WENO7-P scheme

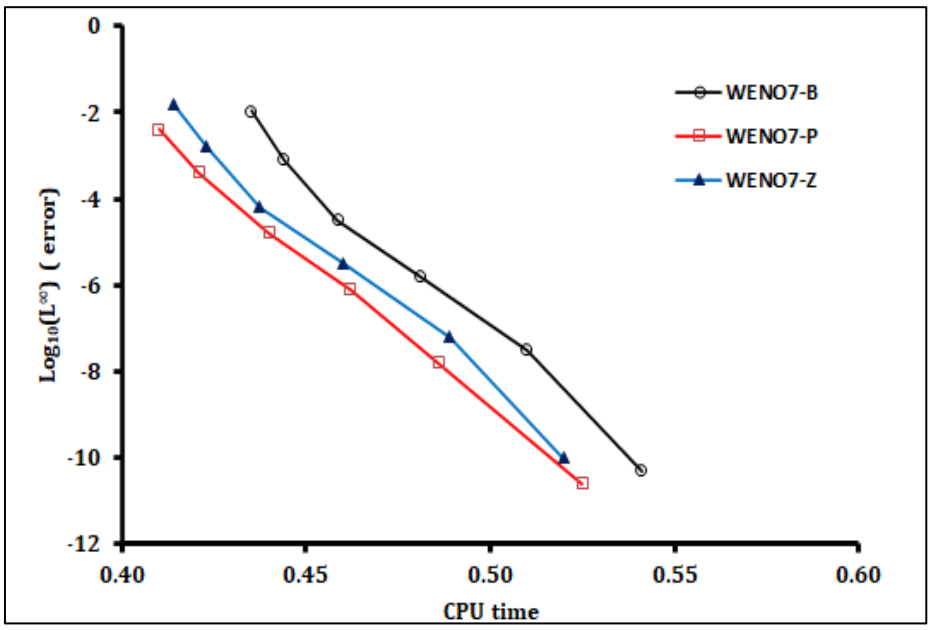

Figure 11: CPU time and L^{∞} curve

Example 7. Shock wave reflection:

Consider a shock is traveling at Mach 3 interacting with density sine waves according to Euler equations

(62); in this case, the shock's initial condition.

$$\begin{aligned}(_L,\ u_L,\ E_L) &= (3.857143,\ 2.629369,\ 10.3333),\quad for\ x < -4,\\ (_R,\ u_R,\ E_R) &= (1 + 0.2\sin 5x,\ 0,\ 1),\quad for\ x > -4.\end{aligned} \tag{64}$$

Physical oscillations in the flow require numerical solutions.

At time interval t=1.8, the solution is found. Figure (12) is a curve displaying the density as calculated by the perturbational technique employing 200 grid points. By making the Comparison between the results generated by WENO7-P with the results of [22, 28], Notice that WENO7-P schemes yield accurate results. To Compare results with other methods, CPU-L^{∞} error curves are shown in figure (13). It is noted that WENO7-P scheme is more efficient.

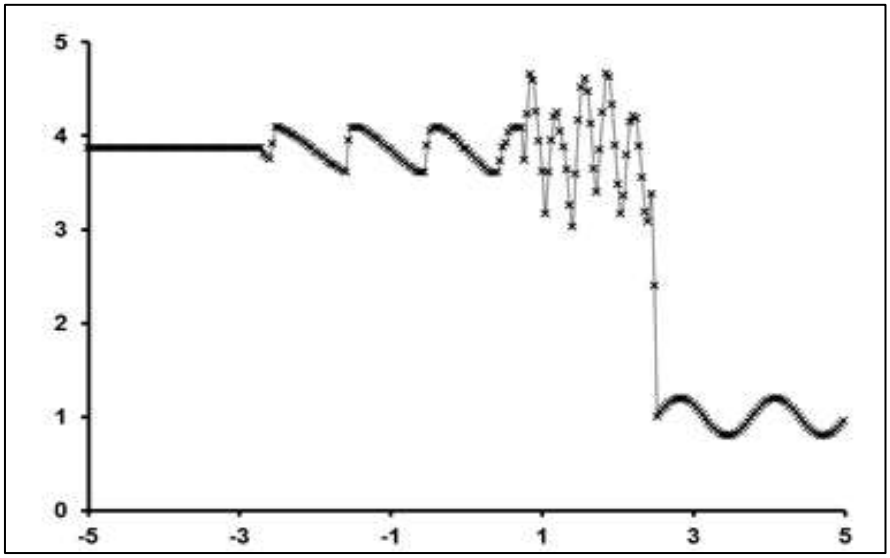

Figure 12: Using WENO7-P scheme

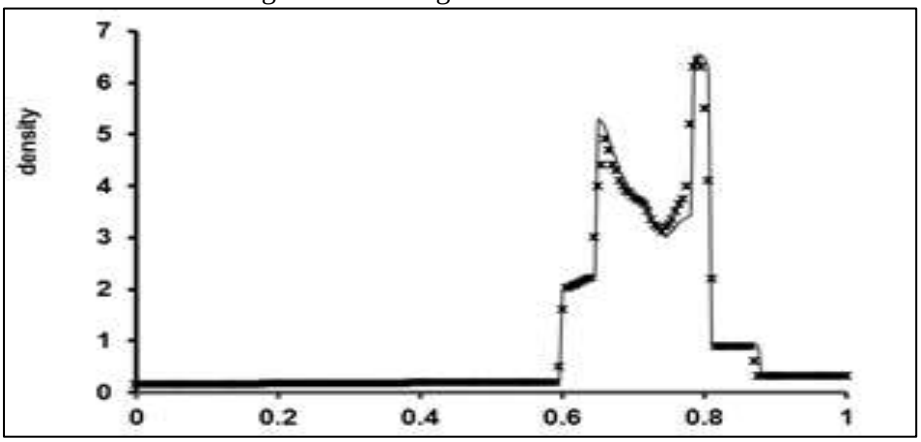

Figure 13: Using WENO7-P scheme

Example 8. The problem of Blast Wave

This problem has three initial states [30].

$$u(x,0) = \begin{cases}(_L,\ u_L,\ P_L) = (1, 0, 1000), & x < 0.1,\\ (_M,\ u_M, P_M) = (1, 0, 0.01), & 0.1 < x < 0.9,\\ (_R,\ u_R,\ P_R) = (1, 0, 100), & x > 0.9.\end{cases} \tag{65}$$

with γ. Both boundaries have reflective boundary conditions. This problem is solved by the propagation of powerful shock waves into regions with low pressure, it contains extremely powerful discontinuities as a benchmark and therefore is a suitable check of schemes. Figure (14) displays the numerical results of this complex problem's density. These results were collected from 200 cells at t = 0.038. In particular,

the peaks of the density have nearly the accurate value, demonstrating that this sharp resolution of the complex and difficult double blast problem is possible with the new scheme

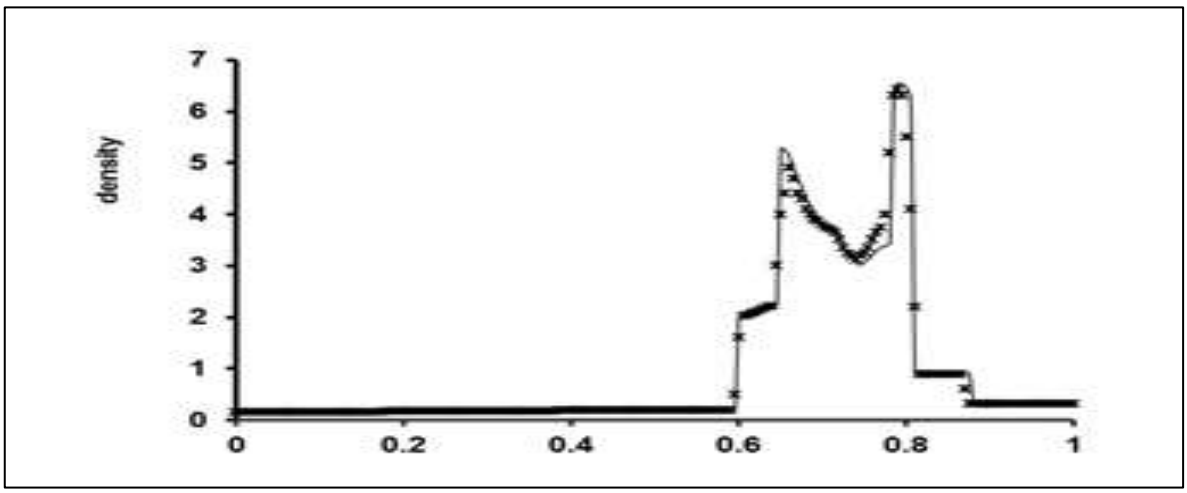

.

Figure 14: Using WENO7-P scheme

6.6 Euler equations in two dimensions

The Euler equations in two dimensions will investigate the WENO7-P scheme's performances of as follows

$$U_t + [F(U)]_y = 0, \tag{66}$$

where

$U = (\rho,\ \rho u,\ v,\ E)^T, F(U) = (\rho u,\ P + u^2 + P,\ uv,\ u(P + E))^T,$

$G(U) = (\rho v,\ uv,\ P + v^2 + P,\ v(P + E))^T$, and $P = (\gamma - 1)[e - 0.5(u^2 + v^2)], S = \frac{P}{\gamma}$

where is the density, P is the pressure, S is the entropy, e is the specific total energy of the fluid, u is the component of x-axis of velocity and v is the component of y-axis of the velocity. γ is the ratio of specific heat and it is assumed that $\gamma = 1.4$.

Example 9. The problem of the Double-Mach reflection

The above-mentioned Euler equations (66) on the $[0,4] \times [0,1]$ are shown in this example to verify the high resolution and numerical stability of the WENO7-P scheme. At the bottom of the domain beginning with $x = \frac{1}{6}$. Positioned using the exact post-shock condition, a right-moving Mach 10 shock makes 60° with the x-axis at $(x, y) = (\frac{1}{6}, 0)$. The bottom boundary is imposed with the exact post-shock condition, while the rest of the x-axis is reflective. Data is used to describe the Mach 10 shock's exact motion at the computational domain's top [30]. It can be seen in Fig. 15 that our scheme generates more instability micro-structure solutions in a shorter amount of time (t=0.2).

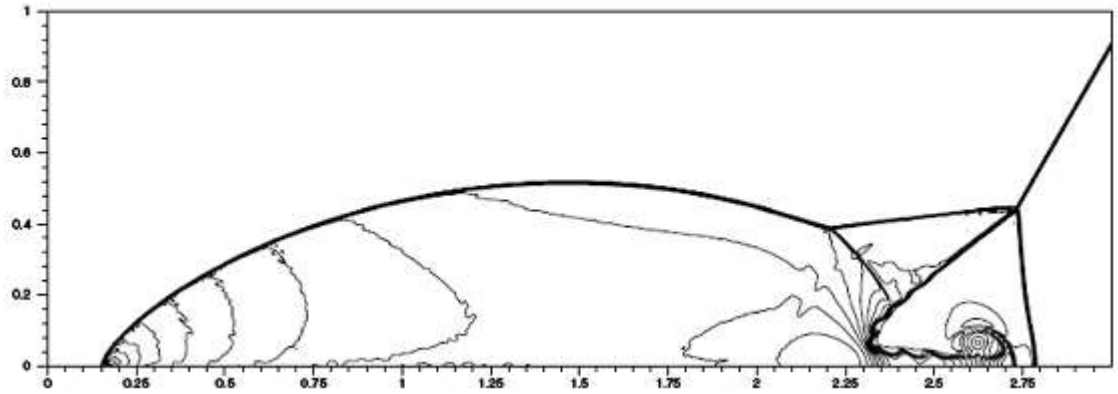

Figure 15: Density contours for the Example 9 by WENO7-P with 30 contour lines with a range from 2 to 22

7. CONCLUSION

Depending on the perturbed polynomials, this research proposes a perturbational weighted essentially non-oscillatory (WENO7-P) scheme. Compared to classical the seventh-order WENO schemes introduced by Henrick et al. and Balsara et al., this one is one order lower, and is less dissipative and dispersive than the WENO scheme. The theoretical analysis and numerical results show that using the same weights as in the WENO7-Z scheme can recover 7th-order at the critical points. According to various results, the WENO7-P scheme is less dissipative and dispersive than the WENO scheme.
Future research should focus on improving the higher-order finite-difference traditional WENO schemes.

8. REFERENCES

[1] F. Zeng, Y. Shen, and S. Liu, "A perturbational weighted essentially non-oscillatory scheme," Computers & Fluids, vol. 172, pp. 196–208, 2018. https://doi.org/10.1016/j. compfluid.2018.07.003.

[2] A. K. Henrick, T. D. Aslam, and J. M. Powers, "Mapped weighted essentially non-oscillatory schemes: achieving optimal order near critical points," Journal of Computational Physics, vol. 207, no. 2, pp. 542–567, 2005. https://doi.org/10.1016/j.jcp.2005.01.023.

[3] R. Borges, M. Carmona, B. Costa, and W. S. Don, "An improved weighted essentially nonoscillatory scheme for hyperbolic conservation laws," Journal of Computational Physics, vol. 227, no. 6, pp. 3191–3211, 2008. DOI:10.1016/j.jcp.2007.11.038.

[4] A. Harten, "High resolution schemes for hyperbolic conservation laws," Journal of computational physics, vol. 135, no. 2, pp. 260–278, 1997. https://doi.org/10.1016/ 0021-9991(83)90136-5.

[5] X.-D. Liu, S. Osher, and T. Chan, "Weighted essentially non-oscillatory schemes," Journal of computational physics, vol. 115, no. 1, pp. 200–212, 1994. https://doi.org/10.1006/ jcph.1994.1187.

[6] G.-S. Jiang and C.-W. Shu, "Efficient implementation of weighted eno schemes," Journal of computational physics, vol. 126, no. 1, pp. 202–228, 1996. https://doi.org/10.1006/ jcph.1996.0130.

[7] S. Zhao, N. Lardjane, and I. Fedioun, "Comparison of improved finite-difference weno schemes for the implicit large eddy simulation of turbulent non-reacting and reacting high-speed shear flows," Computers & Fluids, vol. 95, pp. 74–87, 2014. DOI:10.1016/J.COMPFLUID.2014. 02.017.

[8] P. Fan, Y. Shen, B. Tian, and C. Yang, "A new smoothness indicator for improving the weighted essentially non-oscillatory scheme," Journal of Computational Physics, vol. 269, pp. 329–354, 2014. DOI:10.1016/j.jcp.2014.03.032.

[9] S. Liu, Y. Shen, F. Zeng, and M. Yu, "A new weighting method for improving the weno-z scheme,"

International Journal for Numerical Methods in Fluids, vol. 87, no. 6, pp. 271–291, 2018. https://doi.org/10.1002/fld.4490.

[10] W.-S. Don and R. Borges, "Accuracy of the weighted essentially non-oscillatory conservative finite difference schemes," Journal of Computational Physics, vol. 250, pp. 347–372, 2013. https://doi.org/10.1016/j.jcp.2013.05.018.

[11] M. Castro, B. Costa, and W. S. Don, "High order weighted essentially non-oscillatory weno-z schemes for hyperbolic conservation laws," Journal of Computational Physics, vol. 230, no. 5, pp. 1766–1792, 2011. https://doi.org/10.1016/j.jcp.2010.11.028.

[12] I. Cravero and M. Semplice, "On the accuracy of weno and cweno reconstructions of third order on nonuniform meshes," Journal of Scientific Computing, vol. 67, no. 3, pp. 1219–1246, 2016. DOI:10.1007/s10915-015-0123-3.

[13] Z. Gao et al., "An infinite-order accurate upwind compact difference scheme for the convective diffusion equation," in Proc. of Asia Workshop on Computational Fluid Dynamics, pp. 50–56, Sichuan, China, 1994. https://tex.stackexchange.com/questions/317900/ how-to-use-inproceedings.

[14] Y.-Q. Shen, Z. Gao, and D.-H. Yang, "Second-order perturbational finite difference schemes for hyperbolic conservation equation.," Acta Aerodynamica Sinica, vol. 21, no. 3, pp. 342–350,2003.https://www.semanticscholar. org/paper/Second-order-perturbational-finite-difference-for-Yi/ a09cbcc16780e21a0a0ef850e473a8fc24ba7353.

[15] G. Zhi and Y. Guowei, "Perturbation finite volume method for convective-diffusion integral equation," Acta Mechanica Sinica, vol. 20, no. 6, pp. 580–590, 2004. DOI:10.1007/ BF02485861.

[16] M.-j. Li, Y.-y. Yang, and S. Shu, "Third-order modified coefficient scheme based on essentially non-oscillatory scheme," Applied Mathematics and Mechanics, vol. 29, no. 11, pp. 1477–1486, 2008. DOI:10.1007/S10483-008-1108-X.

[17] C. Yu, Z. Gao, and T. W. Sheu, "Development of a symplectic and phase error reducing perturbation finite-difference advection scheme," Numerical Heat Transfer, Part B: Fundamentals, vol. 70, no. 2, pp. 136–151, 2016. DOI:10.1080/10407790.2015.1097241.

[18] C.-W. Shu and S. Osher, "Efficient implementation of essentially non-oscillatory shockcapturing schemes, ii," in Upwind and High-Resolution Schemes, pp. 328–374, Springer, 1989. https://doi.org/10.1016/0021-9991(88)90177-5.

[19] N. Takemitsu, "Finite difference method to solve incompressible fluid flow," Journal of Computational Physics, vol. 61, no. 3, pp. 499–518, 1985. DOI:10.1016/0021-9991(85)90077-4.

[20] A. Kurganov, S. Noelle, and G. Petrova, "Semidiscrete central-upwind schemes for hyperbolic conservation laws and hamilton–jacobi equations," SIAM Journal on Scientific Computing, vol. 23, no. 3, pp. 707–740, 2001. DOI:10.1137/S1064827500373413.

[21] A. Roman'kov and E. Romenskii, "A runge-kutta/weno method for solving equations for smallamplitude wave propagation in a saturated elastic porous medium," Numerical Analysis and Applications, vol. 7, no. 3, pp. 215–226, 2014. DOI:10.1134/S1995423914030045.

[22] D. S. Balsara and C.-W. Shu, "Monotonicity preserving weighted essentially non-oscillatory schemes with increasingly high order of accuracy," Journal of Computational Physics, vol. 160, no. 2, pp. 405–452, 2000. https://doi.org/10.1006/jcph.2000.6443.

[23] C.-W. Shu and S. Osher, "Efficient implementation of essentially non-oscillatory shockcapturing schemes," Journal of computational physics, vol. 77, no. 2, pp. 439–471, 1988. https://doi.org/10.1016/0021-9991(88)90177-5.

[24] Y. H. Zahran, "Very high order improved weno scheme for hyperbolic conservation laws," Comptes Rendus De L Academie Bulgare Des Sciences, vol. 64, no. 10, pp. 1393–1402, 2011.https://www.researchgate.net/publication/266713864_A_very-high-order_improved_WENO_scheme_for_hyperbolic_conservation_laws.

[25] Y. Ha, C. H. Kim, Y. J. Lee, and J. Yoon, "An improved weighted essentially non-oscillatory scheme with a new smoothness indicator," Journal of Computational Physics, vol. 232, no. 1, pp. 68–86, 2013. https://doi.org/10.1016/j.jcp.2012.06.016.

[26] S. Gottlieb, "On high order strong stability preserving runge-kutta and multi step time discretizations," Journal of scientific computing, vol. 25, no. 1, pp. 105–128, 2005. https://doi.org/10.1007/s10915-004-4635-5.

[27] A. Kurganov, G. Petrova, and B. Popov, "Adaptive semidiscrete central-upwind schemes for nonconvex hyperbolic conservation laws," SIAM Journal on Scientific Computing, vol. 29, no. 6, pp. 2381–2401, 2007. https://doi.org/10.1137/040614189.

[28] Y. Shen and G. Zha, "Improved seventh-order weno scheme," in 48th AIAA Aerospace Sciences Meeting Including the New Horizons Forum and Aerospace Exposition, p. 1451, 2010. DOI: 10.2514/6.2010-1451.

[29] Y. H. Zahran and M. M. Babatin, "Improved ninth order weno scheme for hyperbolic conservation laws," Applied Mathematics and Computation, vol. 219, no. 15, pp. 8198–8212, 2013. https://doi.org/10.1016/j.amc.2013.02.020.

[30] G. Capdeville, "A central weno scheme for solving hyperbolic conservation laws on nonuniform meshes," Journal of Computational Physics, vol. 227, no. 5, pp. 2977–3014, 2008. DOI:10.1016/j.jcp.2007.11.029.

[31] P. Woodward and P. Colella, "The numerical simulation of two-dimensional fluid flow with strong shocks," Journal of computational physics, vol. 54, no. 1, pp. 115–173, 1984. https: //doi.org/10.1016/0021-9991(84)90142-6